


Article

Coupled-Channel Analysis of the Process $\gamma\gamma \rightarrow \pi^0\pi^0$

Yury S. Surovtsev ¹, Petr Bydžovský ², Thomas Gutsche ³, Robert Kamiński ⁴, Valery E. Lyubovitskij ^{3,5,6,7,8,*} 
and Miroslav Nagy ⁹

- ¹ Bogoliubov Laboratory of Theoretical Physics, Joint Institute for Nuclear Research, 141980 Dubna, Russia; surovcev@theor.jinr.ru
- ² Nuclear Physics Institute of the AS CR, 25068 Řež, Czech Republic; bydzovsky@ujf.cas.cz
- ³ Institut für Theoretische Physik, Universität Tübingen, Kepler Center for Astro and Particle Physics, Auf der Morgenstelle 14, D-72076 Tübingen, Germany; thomas.gutsche@uni-tuebingen.de
- ⁴ Institute of Nuclear Physics PAS, 31342 Cracow, Poland; robert.kaminski@ifj.edu.pl
- ⁵ Departamento de Física y Centro Científico Tecnológico de Valparaíso-CCTVal, Universidad Técnica Federico Santa María, Casilla 110-V, Valparaíso 2340000, Chile
- ⁶ Millennium Institute for Subatomic Physics at the High-Energy Frontier (SAPHIR) of ANID, Fernández Concha 700, Santiago 7591538, Chile
- ⁷ Department of Physics, Tomsk State University, 634050 Tomsk, Russia
- ⁸ Department of Mathematics, Tomsk Polytechnic University, 634050 Tomsk, Russia
- ⁹ Institute of Physics, SAS, 84511 Bratislava, Slovakia; miroslav.nagy@savba.sk
- * Correspondence: valeri.lyubovitskij@uni-tuebingen.de

Abstract: We study the process $\gamma\gamma \rightarrow \pi^0\pi^0$ involving the principal mechanisms, the structure of its cross section and the role of individual isoscalar-tensor resonances in the saturation of its energy spectrum.

Keywords: pseudoscalar, scalar and tensor mesons; photon; coupled-channel analysis; energy spectrum



Citation: Surovtsev, Y.S.; Bydžovský, P.; Gutsche, T.; Kamiński, R.; Lyubovitskij, V.E.; Nagy, M. Coupled-Channel Analysis of the Process $\gamma\gamma \rightarrow \pi^0\pi^0$. *Particles* **2022**, *5*, 210–224. <https://doi.org/10.3390/particles5030019>

Academic Editors: Armen Sedrakian and Omar Benhar

Received: 30 March 2022

Accepted: 27 June 2022

Published: 30 June 2022

Publisher's Note: MDPI stays neutral with regard to jurisdictional claims in published maps and institutional affiliations.



Copyright: © 2022 by the authors. Licensee MDPI, Basel, Switzerland. This article is an open access article distributed under the terms and conditions of the Creative Commons Attribution (CC BY) license (<https://creativecommons.org/licenses/by/4.0/>).

1. Introduction

The observation of the processes $\gamma\gamma \rightarrow hadrons$ (including $\gamma\gamma \rightarrow \pi^0\pi^0$ by the Crystal Ball [1] and Belle [2,3]) is rather interesting since they involve an immediate transformation of energy to the masses of strongly interacting particles. The importance of this phenomenon is obvious. Therefore, when analyzing data on energy spectrum of cross section of process $\gamma\gamma \rightarrow \pi^0\pi^0$ in addition to determination of dipole and quadrupole polarizabilities of pions (see, e.g., Ref. [4]), it is extremely interesting to study the coupled-channels contributions, including interference phenomena, and also the role of individual resonances in saturation of the energy spectrum of this process.

Generally processes $\gamma\gamma \rightarrow \pi^+\pi^-, \pi^0\pi^0$ were already studied earlier (see, e.g., Refs. [5–9] and references therein), especially after appearance of the experimental data on these reactions [1–3]. In these works one considers productions of pion pairs in annihilation of both real and virtual photons in the dispersion relation approach with imposing various constraints, such as a Mandelstam analyticity and chiral constraints.

For the observed two-photon annihilation the $\pi^0\pi^0$ pairs are produced in the *S*- and *D*-wave states with isospins $I = 0$ and 2. The isoscalar parts dominate significantly. Earlier we have shown [10] that physical resonances, as the scalar and tensor ones, can be considered correctly only in approaches where the *S*-matrix is determined on the multi-sheeted Riemann surface (the isoscalar-scalar resonances on an 8-sheeted surface, isoscalar-tensor ones on a 16-sheeted one). One should keep in mind that the dispersion relations are written on the 2-sheeted Riemann surface. Therefore, we consider this process by allowing for coupled channels. For the process $\gamma\gamma \rightarrow \pi\pi$ with rescattering in the final state the coupled channels are $\gamma\gamma \rightarrow (\pi\pi, K\bar{K}, \eta\eta) \rightarrow \pi\pi$. The amplitudes for the isoscalar *S*-wave three-channel $\pi\pi$ scattering are taken from our model-independent

analysis of data for $\pi\pi \rightarrow \pi\pi, K\bar{K}, \eta\eta$ [11]. Our approach is based on analyticity and unitarity by using a uniformization procedure (for detailed review of this method see, e.g., Refs. [12–14]). For physical applications see Refs. [10–18]. This method allows to study the S -matrix elements in multichannel hadron scattering processes with taking into account a structure of the corresponding Riemann surface. In particular, in the two- and three-channel cases the corresponding S -matrices are determined on the 4- and 8-sheeted Riemann surfaces, respectively, which are transformed onto the uniformization plane by corresponding conformal mappings. Then we have a possibility to represent correctly multichannel resonances by poles (and by corresponding zeros) on all sheets of the Riemann surface.

Our previous combined description of data on the decays of charmonia— $J/\psi \rightarrow \phi(\pi\pi, K\bar{K}), \psi(2S) \rightarrow J/\psi \pi\pi$, and $X(4260) \rightarrow J/\psi \pi^+\pi^-$ —and of bottomonia— $Y(mS) \rightarrow Y(nS)\pi\pi$ ($m > n, m = 2, 3, 4, 5, n = 1, 2, 3$) [15] (where the contributing amplitude of isoscalar S -wave three-channel $\pi\pi$ scattering was directly taken from the analysis of the processes $\pi\pi \rightarrow \pi\pi, K\bar{K}, \eta\eta$ [11])—implied a confirmation of all our earlier results on the scalar mesons. Therefore, when considering the cross section of the process $\gamma\gamma \rightarrow \pi^0\pi^0$, we will keep the parameters of the S -wave three-channel $\pi\pi$ scattering amplitude [11] unchanged, hoping to obtain an additional confirmation of our results on the scalar mesons.

For the D -wave of multi-channel $\pi\pi$ -scattering in $\gamma\gamma \rightarrow \pi\pi$ we will use the results of our 4-channel analysis of the processes $\pi\pi \rightarrow \pi\pi, (2\pi)(2\pi), K\bar{K}, \eta\eta$, where we also considered the $(2\pi)(2\pi)$ channel [16] explicitly. As in the case of the S -wave 3-channel $\pi\pi$ -scattering, here the resonances are represented by poles on the 16-sheeted Riemann surface. The resonance poles are generated by some 4-channel Breit–Wigner forms with a Blatt–Weisskopf barrier factor due to the meson spins.

In the PDG issue 2020 [19] twelve resonances in the isoscalar-tensor meson sector are discussed, $f_2(1270), f_2(1430)^*, f_2'(1525), f_2(1565)^*, f_2(1640)^*, f_2(1810)^*, f_2(1910)^*, f_2(1950), f_2(2010), f_2(2150)^*, f_2(2300)$, and $f_2(2340)$. The resonances denoted with asterisk were omitted from the summary table as they still need an experimental confirmation. There is considered also the state $f_J(2220)$ ($J^{PC} = 2^{++}$ or 4^{++}) which was omitted from the summary table. In our previous analysis of the multichannel $\pi\pi$ scattering with eleven states, performed in 2010 [16], we have not considered the states $f_2(1640), f_2(1910), f_2(2150), f_2(2300)$, and $f_2(2340)$ but have included the states $f_2(1730), f_2(2020), f_2(2240)$, and $f_2(2410)$. Considering these eleven resonances we obtained a satisfactory combined description of data on the D -wave processes $\pi\pi \rightarrow \pi\pi, K\bar{K}, \eta\eta$, explicitly allowing for the $(2\pi)(2\pi)$ channel. The state $f_2(2020)$ practically did not change the description of data but it allowed the interpretation of the $f_2(2000)$ state as a glueball as it was done in Ref. [20] using an approach based on the $1/N_c$ -expansion. In the presented analysis we use these eleven resonances for the isoscalar-tensor meson sector.

The paper is organized as follows. In Section 2 we derive the formalism for taking into account effects of multi-channel $\pi\pi$ scattering in the decay mode $\gamma\gamma \rightarrow \pi^0\pi^0$. First we present some general basic formulas and a model for the process $\gamma\gamma \rightarrow \pi^0\pi^0$, which is a development of the one proposed in Refs. [21,22], however, with allowing for our previous results on the multichannel $\pi\pi$ scattering, that for obtaining correct values for the f_0 -resonance parameters in the analysis of multichannel $\pi\pi$ scattering data it is needed, as minimum, the tree-coupled channel analysis, namely the combined analysis of the data on S -wave processes $\pi\pi \rightarrow \pi\pi, K\bar{K}, \eta\eta$ [17]. Analogously, to obtain the f_2 -resonance parameters, it is needed the four-channel analysis of the data on D -wave processes $\pi\pi \rightarrow \pi\pi, (2\pi)(2\pi), K\bar{K}, \eta\eta$ [16]. Further we outline our model-independent S -matrix approach based on first principles, such as analyticity and unitarity [16]. It was used in calculating the S - and D -wave amplitudes of the above-indicated coupled processes, which are applied in the model for the process $\gamma\gamma \rightarrow \pi^0\pi^0$. Note that for the present it is reasonable not to consider the channel with isospin $I = 2$ because the Born approximation is equal to zero and there are no mesonic resonances with $I = 2$. Taking into account the format of this paper, we avoid the excessive details of formalism, dispatching to the

corresponding references. In Section 3 we show the results of calculations of the cross section energy spectrum of the $\gamma\gamma \rightarrow \pi^0\pi^0$ in the presented model when comparing with the experimental data [1–3]. There are investigated separately contributions of the S - and D -waves, of the individual channels to the energy spectrum. Also we show the calculated energy spectra of the $\gamma\gamma \rightarrow \pi^0\pi^0$ when switching off the individual f_2 resonances, grouped around the energy interval 1.5–1.73 GeV, where our calculations diverge with the data. Since our approach of principle consists in the combined description of this process and of the above-indicated processes of the S - and D -wave multichannel $\pi\pi$ scattering, we carry out and show the results of the combined analysis (for each case of switching off the individual f_2 resonances) of $\gamma\gamma \rightarrow \pi^0\pi^0$, of the isoscalar S -wave processes $\pi\pi \rightarrow \pi\pi, K\bar{K}, \eta\eta$ and of the isoscalar D -wave processes $\pi\pi \rightarrow \pi\pi, (2\pi)(2\pi), K\bar{K}, \eta\eta$. Finally, Section 4 contains our conclusions.

2. Effect of Multi-Channel $\pi\pi$ Scattering in $\gamma\gamma \rightarrow \pi^0\pi^0$

When studying the process $\gamma\gamma \rightarrow \pi^0\pi^0$ we have to include the effect of intermediate states. Since photons couple to charged objects production of $\pi^0\pi^0$ pairs can only occur through the formation of $\pi^+\pi^-$ and K^+K^- pairs in the intermediate states of the final-state rescattering processes. We describe the coupling of photon with charged pseudoscalar mesons based on the vector meson dominance (VMD) model. According to the VMD model, the hadron electromagnetic current is given by the linear combination of individual contributions of vector meson fields [23]:

$$J_\mu(x) = - \left[\frac{m_\rho^2}{2\gamma_\rho} \rho_\mu^0(x) + \frac{m_\omega^2}{2\gamma_\omega} \omega_\mu^0(x) + \frac{m_\phi^2}{2\gamma_\phi} \phi_\mu^0(x) \right], \tag{1}$$

where m_V is the mass of vector mesons ($V = \rho^0, \omega, \phi$). The coupling constants of the photon with vector mesons are determined by the normalization conditions of vector fields:

$$\langle 0 | J_\mu(0) | V \rangle = - \frac{m_V^2}{2\gamma_V} V_\mu.$$

In the SU_3 -symmetry scheme with ideal $\omega - \phi$ meson mixing one has the relations:

$$\gamma_\rho : \gamma_\omega : \gamma_\phi = 1 : 3 : \left(-\frac{3}{\sqrt{2}} \right). \tag{2}$$

For the constants γ_V there are found the following values [24]:

$$\frac{\gamma_\rho^2}{4\pi} = 0.64 \pm 0.05, \quad \frac{\gamma_\omega^2}{4\pi} = 4.8 \pm 0.5, \quad \frac{\gamma_\phi^2}{4\pi} = 2.8 \pm 0.2. \tag{3}$$

The use of the VMD model permits us to understand how the intermediate states are formed in the process $\gamma\gamma \rightarrow \pi^0\pi^0$. According to the VMD hypothesis, one can consider the γ -quant state as a superposition of the ρ^0 -, ω - and ϕ -meson states [25]:

$$|\gamma\rangle = \sqrt{\alpha\pi} \left(\gamma_\rho^{-1} |\rho^0\rangle + \gamma_\omega^{-1} |\omega\rangle - \gamma_\phi^{-1} |\phi\rangle \right). \tag{4}$$

It is seen that in the $\gamma\gamma$ annihilation the $\rho^0\rho^0$ components are responsible for production of two pairs of charged pions ($\pi^+\pi^-$), the $\phi\phi$ for (K^+K^-), and $\omega\omega$ for two triplets ($\pi^+\pi^-\pi^0$). At that, it is assumed that two opposite-charge mesons (each from the different pairs/triplets of particles, produced by different photons) are paired into t -channel propagator, giving the nearest mesons, exchanged in the crossing-channels. Then in the intermediate states we have two/four pseudoscalar mesons. The VMD relations [see Equations (2) and (3)] are used to define the coupling which is attached to the correspond-

ing diagrams describing the processes $\gamma + \gamma \rightarrow \rho^0 + \rho^0 \rightarrow \pi^+ + \pi^-$, $\gamma + \gamma \rightarrow \phi + \phi \rightarrow K^+ + K^-$, $\gamma + \gamma \rightarrow \omega + \omega \rightarrow 2\pi^+ + 2\pi^-$, and $\gamma + \gamma \rightarrow \omega + \omega \rightarrow \pi^+ + \pi^- + 2\pi^0$.

The cross section of process $\gamma\gamma \rightarrow \pi^0\pi^0$ is written via the helicity amplitudes M_{++} and M_{+-} (the subscripts label the helicities of the incoming photons) [26,27] as follows

$$\frac{d\sigma}{d\Omega} = \frac{1}{256\pi^2s} \sqrt{\frac{s - 4m_\pi^2}{s}} (|M_{++}|^2 + |M_{+-}|^2), \tag{5}$$

where $s = (k_1 + k_2)^2$ with k_1 and k_2 being the 4-momenta of the photons. These helicity amplitudes are decomposed into partial waves:

$$M_{++}(s, \theta, \phi) = e^2 \sqrt{16\pi} \sum_{J \geq 0} F_{J0}(s) Y_{J0}(\theta, \phi), \tag{6}$$

$$M_{+-}(s, \theta, \phi) = e^2 \sqrt{16\pi} \sum_{J \geq 2} F_{J2}(s) Y_{J2}(\theta, \phi). \tag{7}$$

The partial wave amplitudes $F_{J\lambda}$ (helicity $\lambda = 0, 2$) must be determined in the analysis. In the following we do the truncation of the partial wave expansion in Equation (6) by including only the first leading term following the idea proposed in Ref. [22]. This is related to the fact, that in the final state $\pi\pi$ interaction, contributing to the process $\gamma\gamma \rightarrow \pi^0\pi^0$, the S- and D-wave dominate.

In Refs. [21,22] it is argued that the partial amplitudes are approximated in the following form:

$$F_{J\lambda}^{I=0}(\gamma\gamma \rightarrow \pi\pi) = \sum_n a_{J\lambda}^{I=0}(\gamma\gamma \rightarrow n) T_J^{I=0}(n \rightarrow \pi\pi), \tag{8}$$

where the $a_{J\lambda}^{I=0}(\gamma\gamma \rightarrow n)$ approximate transitions from $\gamma\gamma$ to the intermediate states; they are functions of s and real above the $\pi\pi$ threshold. Note that it is reasonable in the case of process $\gamma\gamma \rightarrow \pi^0\pi^0$ not to consider the channel with isospin $I = 2$ because the Born approximation is equal to zero and there are no mesonic resonances with $I = 2$. The $T_J^I(n \rightarrow \pi\pi)$, describing transitions from the intermediate states into pion pair, satisfy the unitarity conditions:

$$\text{Im} T_J^I(n \rightarrow \pi\pi) = \sum_{n'} \rho_n T_J^I(n \rightarrow n')^* T_J^I(n' \rightarrow \pi\pi), \tag{9}$$

where the sum is over the hadronic intermediate states n' , kinematically admitted; ρ_n is the corresponding phase space factor for each channel. When using this relation, one can see, that the expression (8) satisfies the unitarity condition for the amplitude $F_{J\lambda}^I(\gamma\gamma \rightarrow \pi\pi)$ [21,22]:

$$\text{Im} F_{J\lambda}^I(\gamma\gamma \rightarrow \pi\pi) = \sum_n \rho_n F_{J\lambda}^I(\gamma\gamma \rightarrow n)^* T_J^I(n \rightarrow \pi\pi), \tag{10}$$

Considering S-wave multichannel $\pi\pi$ scattering in the final $\pi^0\pi^0$ state, we shall deal with the 3-channel case, i.e. with the reactions $\pi\pi \rightarrow \pi\pi, K\bar{K}, \eta\eta$. In Ref. [17] it was shown that this is a minimal number of coupled channels needed to obtain correct values for the f_0 -resonance parameters in the analysis of multichannel $\pi\pi$ scattering data. For the D-wave multichannel $\pi\pi$ scattering one ought to consider, as minimum, four coupled channels: $\pi\pi \rightarrow \pi\pi, (2\pi)(2\pi), K\bar{K}, \eta\eta$ [16]. We use the following relation between the T-matrix and S-matrix $(T_0^0)_{ij} = \sqrt{s}/(4ik) [(S_0^0)_{ij} - 1]$. Therefore, redenoting in Equation (8) $a_{J=0\lambda=0}^{I=0}(\gamma\gamma \rightarrow n) \equiv a(\gamma\gamma \rightarrow n)$ and $a_{J=2\lambda=2}^{I=0}(\gamma\gamma \rightarrow n) \equiv b(\gamma\gamma \rightarrow n)$, we write the S- and D-wave amplitudes as

$$\begin{aligned}
 F_{00}^{I=0}(\gamma\gamma \rightarrow \pi^0\pi^0) &= a(\gamma\gamma \rightarrow \pi^+\pi^-)T_0^{I=0}(\pi^+\pi^- \rightarrow \pi^0\pi^0) \\
 &+ a(\gamma\gamma \rightarrow K^+K^-)T_0^{I=0}(K^+K^- \rightarrow \pi^0\pi^0) \\
 &+ a(\gamma\gamma \rightarrow \eta\eta)T_0^{I=0}(\eta\eta \rightarrow \pi^0\pi^0), \tag{11}
 \end{aligned}$$

$$\begin{aligned}
 F_{22}^{I=0}(\gamma\gamma \rightarrow \pi^0\pi^0) &= b(\gamma\gamma \rightarrow \pi^+\pi^-)T_2^{I=0}(\pi^+\pi^- \rightarrow \pi^0\pi^0) \\
 &+ b(\gamma\gamma \rightarrow 2\pi^+2\pi^-)T_2^{I=0}(2\pi^+2\pi^- \rightarrow \pi^0\pi^0) \\
 &+ b(\gamma\gamma \rightarrow K^+K^-)T_2^{I=0}(K^+K^- \rightarrow \pi^0\pi^0) \\
 &+ b(\gamma\gamma \rightarrow \eta\eta)T_2^{I=0}(\eta\eta \rightarrow \pi^0\pi^0), \tag{12}
 \end{aligned}$$

where

$$\begin{aligned}
 a(\gamma\gamma \rightarrow \pi^+\pi^-) &= \frac{\alpha_{10}}{(s - \gamma_1)^2} + \alpha_{11} + \alpha_{12}s, \\
 a(\gamma\gamma \rightarrow K^+K^-) &= \frac{\beta_{20}}{(s - \gamma_2)^2} + \beta_{21} + \beta_{22}s, \\
 a(\gamma\gamma \rightarrow \eta\eta) &= \beta_{31} + \beta_{32}s, \\
 b(\gamma\gamma \rightarrow \pi^+\pi^-) &= \frac{\delta_{10}}{(s - \rho_1)^2} + \delta_{11} + \delta_{12}s, \tag{13} \\
 b(\gamma\gamma \rightarrow 2\pi^+2\pi^-) &= \frac{\delta_{20}}{(s - \rho_2)^2} + \delta_{21} + \delta_{22}s, \\
 b(\gamma\gamma \rightarrow K^+K^-) &= \delta_{31} + \delta_{32}s, \\
 b(\gamma\gamma \rightarrow \eta\eta) &= \delta_{41} + \delta_{42}s
 \end{aligned}$$

with an obvious notation. These parameters must be determined, on the whole, in a combined fit to data on $\gamma\gamma \rightarrow \pi^0\pi^0$ [1–3] and on isoscalar *S*- and *D*-wave multi-channel $\pi\pi$ -scattering. Note that the VMD couplings are absorbed into the parameters α_{11} , α_{12} , β_{21} , β_{22} , δ_{ij} , in Equation (13) and the latter are fitted to data to guarantee that the obtained corresponding values of these couplings approximately satisfy to the relations (2) and (3). Let us explain the pole terms in the coefficients *a* and *b*. Whereas in the direct channel of process $\gamma\gamma \rightarrow \pi\pi$ the isoscalar-scalar and isoscalar-tensor meson resonances contribute, in the crossing-channels (the Compton scattering $\gamma\pi \rightarrow \gamma\pi$) other resonances contribute: from the nearest – exchanges of the $\rho(770)$, $\omega(782)$, $\phi(1020)$, $b_1(1235)$, $a_1(1260)$ and $a_2(1320)$. We approximate these exchanges effectively by the pole term determined in the analysis. Also the pole term in $a(\gamma\gamma \rightarrow K^+K^-)$ approximates the *K*-meson exchange in the K^+K^- intermediate state between the γK^+ and γK^- vertices; the pole terms in $b(\gamma\gamma \rightarrow \pi^+\pi^-)$ and in $b(\gamma\gamma \rightarrow 2\pi^+2\pi^-)$ arise from pion exchanges in the $\pi^+\pi^-$ and 4π intermediate states, respectively, between the $\gamma\pi^+$ and $\gamma\pi^-$ vertices and between the $\gamma 2\pi$ vertices. Note that the appearance of the 2nd-order poles is related with the fact that both channels, being crossing with respect to the direct channels, coincide with each other.

We further complement our previous satisfactory combined description of data on the decays of charmonia – $J/\psi \rightarrow \phi(\pi\pi, K\bar{K})$, $\psi(2S) \rightarrow J/\psi \pi\pi$ and $X(4260) \rightarrow J/\psi \pi^+\pi^-$, of bottomonia – $Y(mS) \rightarrow Y(nS)\pi\pi$ ($m > n$, $m = 2, 3, 4, 5$, $n = 1, 2, 3$) and of isoscalar *S*-wave processes $\pi\pi \rightarrow \pi\pi, K\bar{K}, \eta\eta$ [15] also by the description of $\gamma\gamma \rightarrow \pi^0\pi^0$ and of isoscalar *D*-wave four-channel $\pi\pi$ scattering ($\pi\pi \rightarrow \pi\pi, (2\pi)(2\pi), K\bar{K}, \eta\eta$). Therefore, the parameters of isoscalar-scalar and isoscalar-tensor resonances, obtained in our earlier analyses [16], remain unchanged. We also intend to investigate the role of individual resonances (in the first turn the isoscalar-tensor mesons) in the saturation of the energy spectrum of $\gamma\gamma \rightarrow \pi^0\pi^0$.

We first outline our model-independent *S*-matrix approach based on first principles, such as analyticity and unitarity [16]. It was used in our analysis of isoscalar *S*- and *D*-wave $\pi\pi$ scattering. This approach had the most success for the *S*-wave scattering in the two- and three-channel cases, because 4- and 8-sheeted Riemann surfaces, on which the corre-

sponding S -matrices are determined, respectively, are transformed onto the uniformization plane by a conformal mapping (in three-channel case by neglecting the $\pi\pi$ -threshold branch point [18]). With $S = S_{bgr}S_{res}$, where S_{bgr} is the background part, S_{res} represents the contribution of resonances which is parameterized on the uniformization plane by poles and corresponding zeros without additional assumptions [13]. For the parameterisation of S_{res} by poles and zeros it is convenient to use the Le Couteur-Newton relations [28]:

$$\begin{aligned} S_{ii} &= \frac{d(k_1, \dots, k_{i-1}, -k_i, k_{i+1}, \dots, k_N)}{d(k_1, \dots, k_N)}, \\ S_{ii}S_{jj} - S_{ij}^2 &= \frac{d(k_1, \dots, k_{i-1}, -k_i, k_{i+1}, \dots, k_{j-1}, -k_j, k_{j+1}, \dots, k_N)}{d(k_1, \dots, k_N)}. \end{aligned} \tag{14}$$

The Jost matrix determinant $d(k_1, \dots, k_N)$, being a real analytic function (i.e., $d(s^*) = d^*(s)$ for all s), has the only square-root branch-points at the channel momenta $k_i = 0$.

For S -wave $\pi\pi$ scattering, when using the uniformizing variable [18]:

$$w = \frac{\sqrt{(s - s_2)s_3} + \sqrt{(s - s_3)s_2}}{\sqrt{s(s_3 - s_2)}} \quad (s_2 = 4m_K^2 \text{ and } s_3 = 4m_\eta^2) \tag{15}$$

where we have neglected the $\pi\pi$ -threshold branch point and allowed for the $K\bar{K}$ - and $\eta\eta$ -threshold branch points and left-hand branch point at $s = 0$ related to the crossed channels, – the Jost matrix determinant $d(k_1, k_2, k_3)$ is transformed into the branch-point-free function $d(w)$. Parametrization of the $d(w)$ by poles and zeros, representing resonances, and the analysis of three-channel $\pi\pi$ scattering (the result has $\chi^2/\text{ndf} \approx 1.16$) can be found in Refs. [17,18]. Also note, that with the uniformizing variable (15) it is impossible, in principle, to describe a small near- $\pi\pi$ -threshold region in the phase shift of the $\pi\pi$ -scattering amplitude. Therefore, to allow for 10 high-statistics data points for the $\pi\pi$ phase shift in this region from the NA48/2 Collaboration [29], we have continued the phase shift to the $\pi\pi$ -threshold as follows

$$\delta_{11}(s) = \text{ArcSin} \left[2\sqrt{1 - 4m_{\pi^+}^2/s} \left(a_{\pi\pi} + b_{\pi\pi} \frac{s - 4m_{\pi^+}^2}{4m_{\pi^+}^2} \right) \right] \theta(m_0^2 - s) + \overline{\delta}_{11}(s)\theta(s - m_0^2). \tag{16}$$

We use the following set of the parameters. The parameters $a_{\pi\pi}$ and $b_{\pi\pi}$ are fixed as $a_{\pi\pi} = 0.282$ and $b_{\pi\pi} = 0.222$. $m_0 = 0.4115$ GeV is the scale parameter splitting the regions of the s variable into two parts: (1) small near- $\pi\pi$ threshold region and (2) region where the phase shift of the $\pi\pi$ -scattering amplitude $\overline{\delta}_{11}(s)$ was obtained in our earlier model-independent analysis [17,18] without allowing for the near- $\pi\pi$ -threshold data [29]; then m_0 is determined by the smooth sewing of the indicated parts of the phase shift. With the phase shift (16) the satisfactory description of the isoscalar S -wave $\pi\pi$ -scattering (modulus and phase shift of the amplitude) is with $\chi^2/\text{n.d.f.} \approx 1.08$, and of the isoscalar S -wave three-channel $\pi\pi$ -scattering, i.e. of three coupled S -wave channels $\pi\pi \rightarrow \pi\pi, K\bar{K}, \eta\eta$, with $\chi^2/\text{n.d.f.} \approx 1.12$.

When considering isoscalar D -wave multichannel $\pi\pi$ -scattering, we are forced to deal at least with four coupled channels $\pi\pi \rightarrow \pi\pi, (2\pi)(2\pi), K\bar{K}, \eta\eta$, therefore, our method of the uniformizing variable cannot be applied. Here we generated the resonance poles by some four-channel Breit-Wigner forms in the Jost matrix determinant $d(k_1, k_2, k_3, k_4) = d_B d_{res}$, where the resonance part is

$$d_{res}(s) = \prod_r \left[M_r^2 - s - i \sum_{j=1}^4 \rho_{rj}^5 R_{rj} f_{rj}^2 \right]. \tag{17}$$

Here $\rho_{rj} = 2k_j / \sqrt{M_r^2 - 4m_j^2}$, f_{rj}^2 / M_r is the partial width and $k_j = \sqrt{s - 4m_j^2} / 2$ is the j -channel momentum with the channel mass m_j , where $j = 1, 2, 3$, and 4 denotes the $\pi\pi$,

$(2\pi)(2\pi)$, $K\bar{K}$, and $\eta\eta$ channels, respectively. More details can be found in Ref. [16]. For detailed description of the Breit-Wigner method we refer to paper [30].

The Blatt–Weisskopf barrier factor for a tensor particle is

$$R_{rj} = \frac{9 + \frac{3}{4} \left(\sqrt{M_r^2 - 4m_j^2} r_{rj} \right)^2 + \frac{1}{16} \left(\sqrt{M_r^2 - 4m_j^2} r_{rj} \right)^4}{9 + \frac{3}{4} \left(\sqrt{s - 4m_j^2} r_{rj} \right)^2 + \frac{1}{16} \left(\sqrt{s - 4m_j^2} r_{rj} \right)^4}, \quad (18)$$

with radii r_{rj} of 0.943 fm for all resonances in all channels except for $f_2(1270)$ and $f_2(1960)$. In particular, for $f_2(1270)$: 1.498, 0.708, and 0.606 fm in the channels $\pi\pi$, $K\bar{K}$, and $\eta\eta$, respectively; for $f_2(1960)$: 0.296 fm in the channel $K\bar{K}$. The description of the accessible data on isoscalar D -wave four-channel $\pi\pi$ scattering ($\pi\pi \rightarrow \pi\pi, (2\pi)(2\pi), K\bar{K}, \eta\eta$) [31,32] results in $\chi^2/\text{n.d.f.} \approx 1.58$.

3. Numerical Results

With the obtained amplitudes of isoscalar S - and D -wave multi-channel $\pi\pi$ -scattering of Equations (11) and (12) we also obtain a satisfactory description of the cross sections for $\gamma\gamma \rightarrow \pi^0\pi^0$. The fit to the data from the Crystal Ball [1] and Belle [2,3] Collaborations in the energy region from the $\pi\pi$ threshold to ≈ 2.23 GeV has a χ^2 , averaged on the number of experimental points, of $\chi^2/\text{n.p.} \approx 1.30$.

The free parameters in Equations (13) are found to be $\alpha_{10} = -4.39948$, $\gamma_1 = -2.414$, $\alpha_{20} = 56.97042$, $\alpha_{30} = -13.64394$; $\beta_{20} = 0.33308$, $\gamma_2 = 0.02913$, $\beta_{21} = -150.47327$, $\beta_{22} = 148.66336$; $\beta_{31} = -121.01348$, $\beta_{32} = 93.55851$; $\delta_{10} = 320.91310$, $\rho_1 = 0.075394$, $\delta_{11} = 720.63174$, $\delta_{12} = -166.62981$; $\delta_{20} = 35.65701$, $\rho_2 = 0.075394$, $\delta_{21} = 182.68994$, $\delta_{22} = -42.44117$; $\delta_{31} = 31.15567$, $\delta_{32} = -6.46263$; $\delta_{41} = 783.32892$, $\delta_{42} = -200.53452$. Note that, e.g., the parameters $\delta_{10} = 320.91310$ and $\delta_{20} = 35.65701$, related to isovector and isoscalar components of the hadron electromagnetic current (1), respectively, satisfy approximately the corresponding relation (2).

Considering (with the determined parameters) the quantities $a(\gamma\gamma \rightarrow n)$ and $b(\gamma\gamma \rightarrow n)$, which describe transitions to the final $\pi^0\pi^0$ state through the corresponding intermediate states $n = \pi^+\pi^-, 2\pi^+2\pi^-, K^+K^-, \eta\eta$, one can conclude, that the contribution of isoscalar D -wave multi-channel $\pi\pi$ scattering is dominant in comparison to the S -wave one. This could be expected when considering the data for the energy spectrum with a large enhancement in the $f_2(1270)$ region.

In Figure 1 we present our description of data on the energy spectrum of cross section of $\gamma\gamma \rightarrow \pi^0\pi^0$ from the Crystal Ball [1] and Belle [2,3] Collaborations. In Figure 1a we compare full results (solid line) with separate contributions from the S (long-dashed line)- and D (dotted line)-waves. Note, the energy spectrum of $\gamma\gamma \rightarrow \pi^0\pi^0$ from the $\pi\pi$ -threshold to the $K\bar{K}$ -threshold is almost completely determined by the S -wave and above the $K\bar{K}$ -threshold (and especially above ≈ 1.3 GeV) by the D -wave contribution. The observed bell-shaped behaviour of the energy spectrum in the near- $\pi\pi$ -threshold region is related to the S -wave contribution, whereas dips and structures above 1.3 GeV are due to the f_2 -resonances contributing to the D -wave including their interference. In Figure 1b we display the comparison of full result (solid line) with contributions of the individual coupled channels — $\pi\pi$ channel (long-dashed line), $K\bar{K}$ channel (dotted line), $\eta\eta$ channel (short-dashed line). One should stress that the bell-shaped behaviour of the near- $\pi\pi$ -threshold energy spectrum is mainly related to the S -wave $K\bar{K}$ intermediate state contribution. We also observe a sizable contribution of the D -wave process $\gamma\gamma \rightarrow \pi^+\pi^- \rightarrow \pi^0\pi^0$. Above ≈ 0.85 GeV we also get a noticeable contribution of the D -wave process $\gamma\gamma \rightarrow \eta\eta \rightarrow \pi^0\pi^0$ (in comparison with the ones of the other coupled processes $\gamma\gamma \rightarrow K^+K^- \rightarrow \pi^0\pi^0$ and $\gamma\gamma \rightarrow (\pi^+\pi^-)(\pi^+\pi^-) \rightarrow \pi^0\pi^0$). The large contribution of the one-pion exchange to the crossing channel of the D -wave process $\gamma\gamma \rightarrow \pi\pi \rightarrow \pi\pi$ is expected. The intermediate state $\eta\eta$ in the reaction $\gamma\gamma \rightarrow \pi^0\pi^0$ implies, of course, a preceding pair of charged particles ($\pi^+\pi^-$) in the intermediate state, that is, the process $\gamma\gamma \rightarrow \pi^+\pi^- \rightarrow \eta\eta \rightarrow \pi^0\pi^0$ and

the one-pion exchange between the $\gamma\pi^+$ and $\gamma\pi^-$ vertices. In any case, this explains the noticeable contribution of the D -wave process $\gamma\gamma \rightarrow \eta\eta \rightarrow \pi^0\pi^0$.

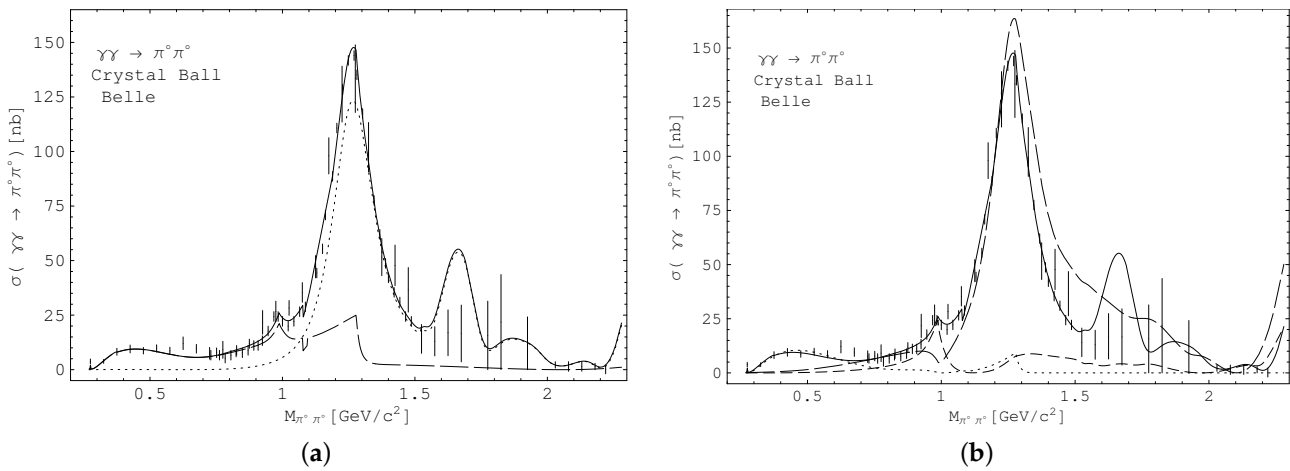


Figure 1. Description of the cross section of the $\gamma\gamma \rightarrow \pi^0\pi^0$ process. The experimental data are taken from the Crystal Ball [1] and Belle [2,3] Collaborations. (a): Full result for the cross section (solid line) is compared with contributions of the S -wave (long-dashed line) and D -wave (dotted line). (b): Full result for the cross section (solid line) is compared with contributions of the coupled channels to the calculated energy spectrum by the $\pi\pi$ channel (long-dashed line); $K\bar{K}$ channel (dotted line); $\eta\eta$ channel (short-dashed line).

From Figure 1 it is evident that data of the Crystal Ball [1] and Belle [2,3] Collaborations are quite consistent. Though the Belle Collaboration data are only available from 0.73 to 1.49 GeV, the Crystal Ball data reside in the energy range from the $\pi\pi$ threshold up to ≈ 2.22 GeV, however they have rather big statistical errors. It is also seen that there is some discrepancy between our calculations and the experimental energy spectrum in interval from ≈ 1.5 to ≈ 1.73 GeV. Therefore, keeping in mind the uncertain status of a number of isoscalar-tensor mesons (six among twelve mesons, indicated in the PDG issue [19], need confirmation), it is worth considering the role of individual resonances (being situated in the interval from 1.5 to 1.73 GeV) in the saturation of the energy spectrum of $\gamma\gamma \rightarrow \pi^0\pi^0$. These are the resonances $f_2(1534.7)$, $f_2(1601.5)$, $f_2(1719.8)$, and $f_2(1760)$.

We would like to stress, that the obtained quite satisfactory description of data on the energy spectrum of $\gamma\gamma \rightarrow \pi^0\pi^0$ cross section jointly with the satisfactory combined description of data on the isoscalar S -wave three-channel $\pi\pi$ scattering ($\pi\pi \rightarrow \pi\pi, K\bar{K}, \eta\eta$), on the isoscalar D -wave four-channel $\pi\pi$ scattering ($\pi\pi \rightarrow \pi\pi, (2\pi)(2\pi), K\bar{K}, \eta\eta$) and on the above-indicated decays of charmonia and bottomonia [15] successfully confirms all our preceding results on scalar mesons obtained in Ref. [11].

Next we consider the role of individual isoscalar-tensor mesonic resonances in saturation of the energy spectrum of the process $\gamma\gamma \rightarrow \pi^0\pi^0$. It is worth making, because interval 1.5–1.73 GeV, where our calculations diverge with the data [see Figure 1b], are in the region described mainly by the D -wave.

Further, switching off the f_2 resonances, grouped around the energy interval 1.5–1.73 GeV, we have performed a combined analysis (for each case) of $\gamma\gamma \rightarrow \pi^0\pi^0$, of the isoscalar S -wave processes $\pi\pi \rightarrow \pi\pi, K\bar{K}, \eta\eta$, and of the isoscalar D -wave processes $\pi\pi \rightarrow \pi\pi, (2\pi)(2\pi), K\bar{K}, \eta\eta$. In Table 1 we make correspondence of the omitted resonances in the Particle Data Group (PDG) [19] with our predictions. In the following we use the notations for the resonances $f_J(M_{\text{our}})$, where M_{our} is our prediction for the mass of the corresponding state. In Table 2 we list $\chi^2/\text{n.p.}$, for the former description of decay processes and the total $\chi^2/\text{n.d.f.}$, calculated for the combined analyses also for each case.

Table 1. Correspondence of the omitted f_2 resonances in the PDG [19] with our predictions.

PDG [19]	$f_2(1430)$	$f_2(1565)$	$f_2(1640)$	$f_2(1810)$	$f_2(1910)$	$f_2(2150)$
Our predictions	$f_2(1450.5)$	$f_2(1534.7)$	$f_2(1601.5)$	$f_2(1719.8)$	$f_2(1760.0)$	$f_2(2202.0)$

Table 2. χ^2 analysis.

Omitted State	–	$f_2(1450.5)$	$f_2(1534.7)$	$f_2(1601.5)$	$f_2(1719.8)$	$f_2(1760.0)$	$f_2(2202.0)$
$\chi^2/n.p.$	1.30	1.50	1.51	1.47	1.53	1.51	1.52
total $\chi^2/n.d.f.$	1.32	1.51	1.36	1.51	1.58	1.48	1.44
Omitted states	$f_2(1430)$ & $f_2(1534.7)$	$f_2(1534.7)$ & $f_2(1601.5)$	$f_2(1534.7)$ & $f_2(1719.8)$	$f_2(1534.7)$ & $f_2(1760)$	$f_2(1601.5)$ & $f_2(1719.8)$	$f_2(1601.5)$ & $f_2(1760)$	$f_2(1719.8)$ & $f_2(1760)$
$\chi^2/n.p.$	1.56	1.35	1.51	1.53	1.17	1.47	1.22
total $\chi^2/n.d.f.$	1.52	1.54	1.58	1.48	1.81	1.61	1.60

In Figure 2 we show our predictions for the cross section of the $\gamma\gamma \rightarrow \pi^0\pi^0$ process for different scenarios, when relevant tensor mesons (f_2 -resonances) are switched off from the analysis. In particular, in Figure 2a we present the comparison of the following scenarios: (1) full result with taking into account of all involved f_0 - and f_2 -resonances (solid line); (2) $f_2(1450.5)$ state is excluded (dotted line); (3) $f_2(1601.5)$ state is excluded (short-dashed line); (4) $f_2(1534.7)$ state is excluded (long-dashed line). In Figure 2b we make comparison of the scenarios: (1) full result with taking into account of all involved f_0 - and f_2 -resonances (solid line); (2) $f_2(1719.8)$ state is excluded (dotted line); (3) $f_2(2202)$ state is excluded (short-dashed line); (4) $f_2(1760)$ state is excluded (long-dashed line). Then, in Figure 2c we display the results for the scenarios: (1) $f_2(1450.5)$ and $f_2(1534.7)$ states are excluded (solid line); (2) $f_2(1534.7)$ and $f_2(1719.8)$ states are excluded (dotted line); (3) $f_2(1534.7)$ and $f_2(1601.5)$ states are excluded (short-dashed line); (4) $f_2(1534.7)$ and $f_2(1760)$ states are excluded (long-dashed line). Finally, in Figure 2d we compare our predictions for the following scenarios: (1) full result with taking into account of all involved f_0 - and f_2 -resonances (solid line); (2) $f_2(1601.5)$ and $f_2(1719.8)$ states are excluded (dotted line); (3) $f_2(1601.5)$ and $f_2(1760)$ states are excluded (short-dashed line); (4) $f_2(1719.8)$ and $f_2(1760)$ states are excluded (long-dashed line).

The description of data in the energy region from $\pi\pi$ threshold to about 1.45 GeV (and in a short region above 2.04 GeV) is almost the same when turning off the different f_2 contributions. The main differences of the calculated energy dependencies of these variants are situated in the interval from 1.45 to 2.04 GeV.

In Figure 2 we see that in the interval 1.5–1.73 GeV, where the experimental energy spectrum of the process $\gamma\gamma \rightarrow \pi^0\pi^0$ differs considerably from our calculations, the data have rather big experimental errors. Therefore, the coupled-channel method described here is promising for exclusion of particular f_2 mesons once more data are available.

The results in Table 2 show that if the pairs of resonances $f_2(1601.5)$ & $f_2(1719.8)$ and $f_2(1719.8)$ & $f_2(1760)$ are omitted a better fit to the $\gamma\gamma \rightarrow \pi^0\pi^0$ data is obtained ($\chi^2/n.p.$ is smaller: 1.17 and 1.22, respectively) which indicates that these resonances are not important in describing the energy spectra of $\gamma\gamma \rightarrow \pi^0\pi^0$. However, omitting these states results in an unsatisfactory description of the coupled-channel scattering $\pi\pi \rightarrow K\bar{K}, \eta\eta$ ($\chi^2/n.d.f.$ is much larger) and therefore the indicated states cannot be excluded in the combined analysis.

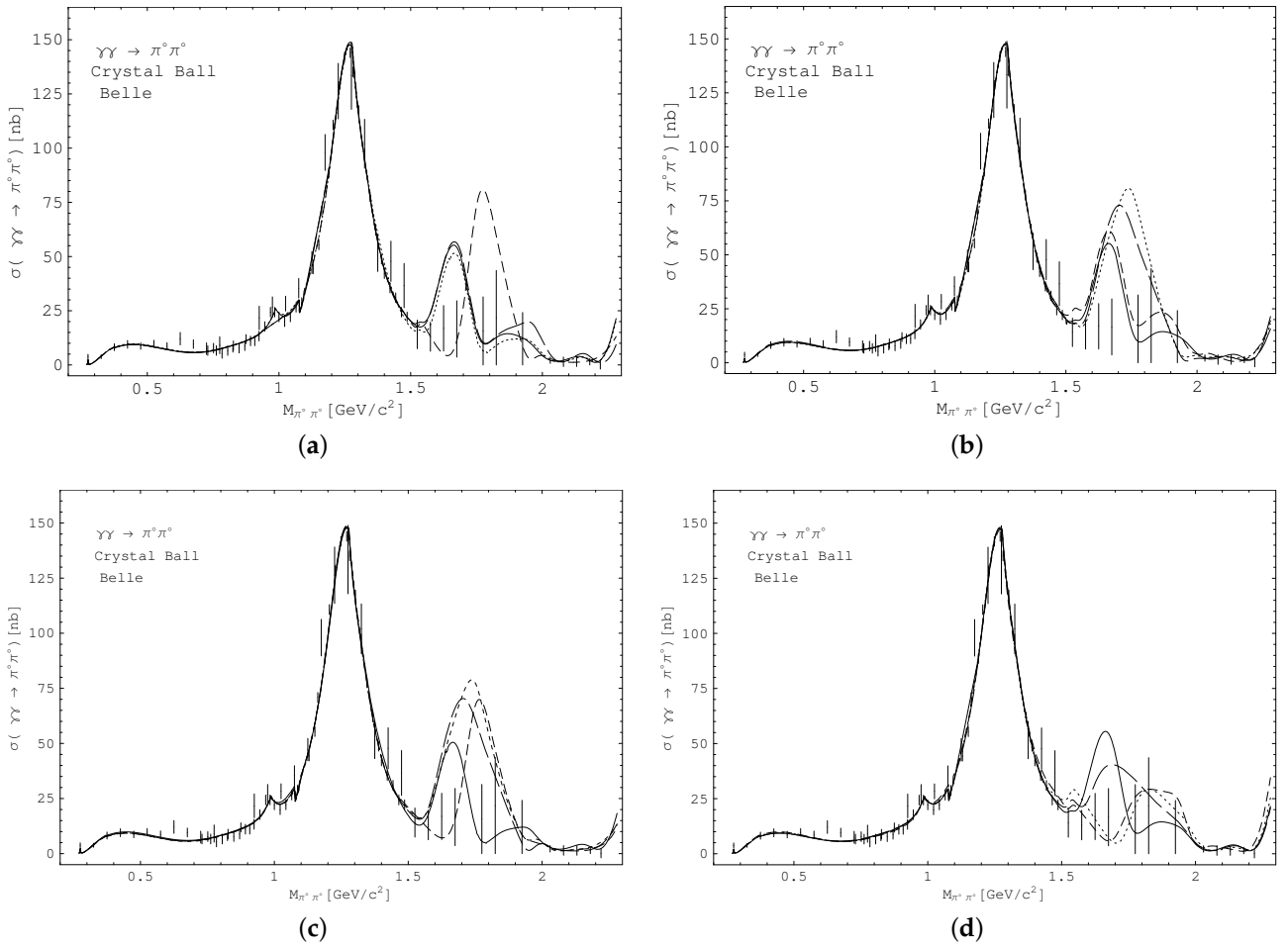


Figure 2. Results for the cross section of the $\gamma\gamma \rightarrow \pi^0\pi^0$ for different scenarios when relevant tensor mesons (f_2 -resonances) are switched off from the analysis. (a): Comparison of the scenarios: (1) full result with taking into account of all involved f_0 - and f_2 -resonances (solid line); (2) $f_2(1450.5)$ state is excluded (dotted line); (3) $f_2(1601.5)$ state is excluded (short-dashed line); (4) $f_2(1534.7)$ state is excluded (long-dashed line). (b): Comparison of the scenarios: (1) full result with taking into account of all involved f_0 - and f_2 -resonances (solid line); (2) $f_2(1719.8)$ state is excluded (dotted line); (3) $f_2(2202)$ state is excluded (short-dashed line); (4) $f_2(1760)$ state is excluded (long-dashed line). (c): Comparison of the scenarios: (1) $f_2(1450.5)$ and $f_2(1534.7)$ states are excluded (solid line); (2) $f_2(1534.7)$ and $f_2(1719.8)$ states are excluded (dotted line); (3) $f_2(1534.7)$ and $f_2(1601.5)$ states are excluded (short-dashed line); (4) $f_2(1534.7)$ and $f_2(1760)$ states are excluded (long-dashed line). (d): Comparison of the scenarios: (1) full result with taking into account of all involved f_0 - and f_2 -resonances (solid line); (2) $f_2(1601.5)$ and $f_2(1719.8)$ states are excluded (dotted line); (3) $f_2(1601.5)$ and $f_2(1760)$ states are excluded (short-dashed line); (4) $f_2(1719.8)$ and $f_2(1760)$ states are excluded (long-dashed line).

Our original aim was to obtain a satisfactory combined description of the reaction $\gamma\gamma \rightarrow \pi^0\pi^0$, of previously investigated decays of charmonia – $J/\psi \rightarrow \phi(\pi\pi, K\bar{K})$, $\psi(2S) \rightarrow J/\psi \pi\pi$, and $X(4260) \rightarrow J/\psi \pi^+\pi^-$ – of bottomonia – $Y(mS) \rightarrow Y(nS)\pi\pi$ ($m > n$, $m = 2, 3, 4, 5$, $n = 1, 2, 3$) [15], and the isoscalar S- and D-wave multi-channel $\pi\pi$ -scattering processes [11]. With respect to the last cases we also carried out calculations for the D-wave processes $\pi\pi \rightarrow \pi\pi, (2\pi)(2\pi), K\bar{K}, \eta\eta$ studying the various variants of the f_2 -resonances. Results are shown in Figures 3–6. In these figures it is seen that the phase shifts of D-wave $\pi\pi$ -scattering are almost the same in all the considered scenarios. All differences in the description of data are encoded in the moduli of the amplitudes of studied processes.

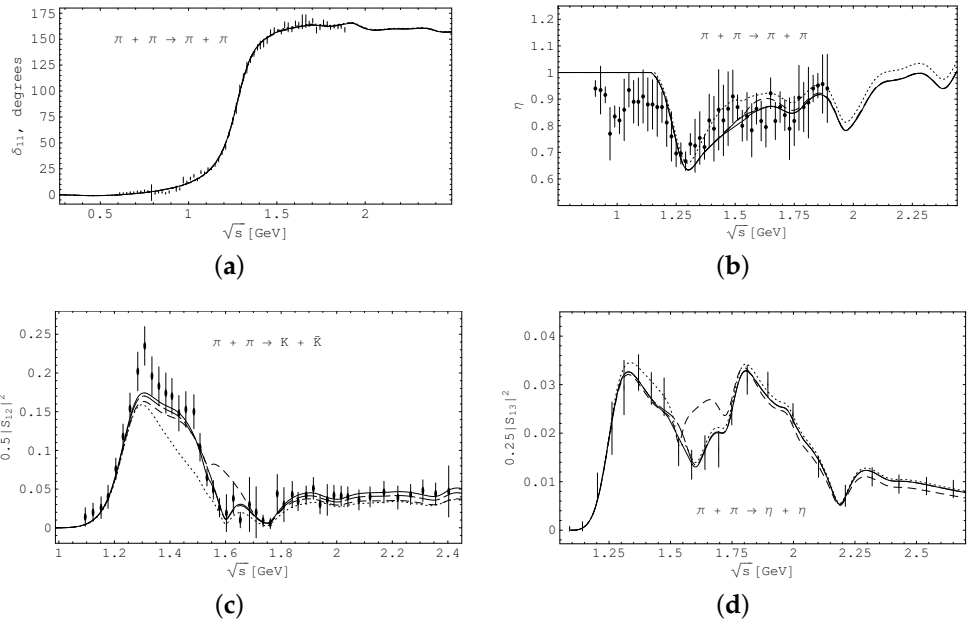


Figure 3. Scattering properties of the $\pi\pi \rightarrow \pi\pi, K\bar{K}, \eta\eta$ processes for four scenarios: (1) full result with inclusion of all relevant f_2 -resonances (solid lines); (2) $f_2(1450.5)$ state is excluded (dotted line); (3) $f_2(1601.5)$ state is excluded (short-dashed line); (4) $f_2(1534.7)$ state is excluded (long-dashed line). (a): Phase shift and in the D -wave $\pi\pi$ -scattering. The experimental data are from Refs. [31,32]. (b): Modulus of the S -matrix element in the D -wave $\pi\pi$ -scattering. (c): Squared moduli of the S -matrix element in the D -wave $\pi\pi \rightarrow K\bar{K}$ process. (d): Squared moduli of the S -matrix element in the D -wave $\pi\pi \rightarrow \eta\eta$ process.

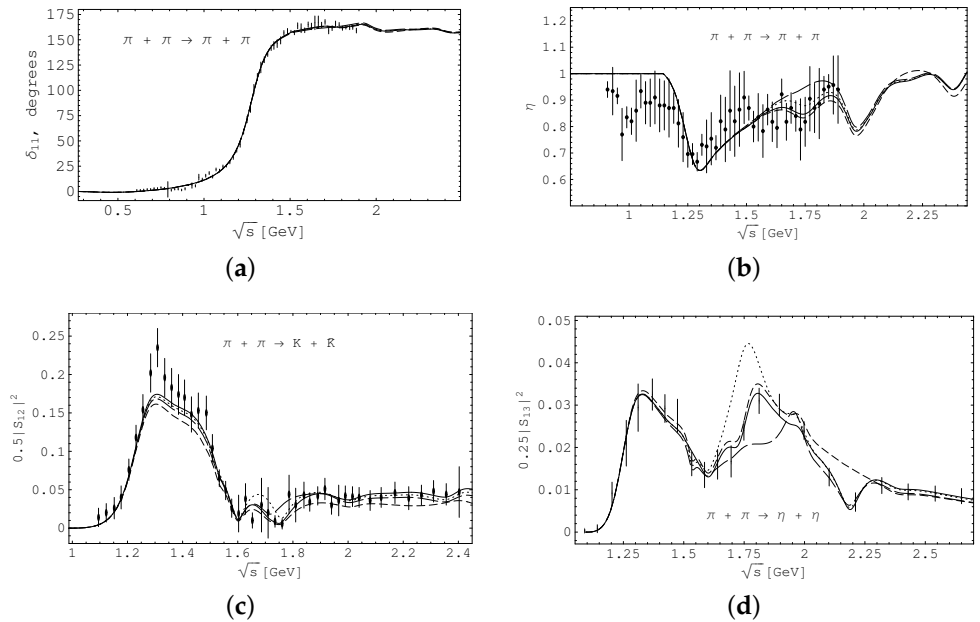


Figure 4. Scattering properties of the $\pi\pi \rightarrow \pi\pi, K\bar{K}, \eta\eta$ processes for four scenarios: (1) full result with inclusion of all relevant f_2 -resonances (solid lines); (2) $f_2(1719.8)$ state is excluded (dotted line); (3) $f_2(2202)$ state is excluded (short-dashed line); (4) $f_2(1760)$ state is excluded (long-dashed line). The experimental data are from Refs. [31,32]. (a): Phase shift and in the D -wave $\pi\pi$ -scattering. (b): Modulus of the S -matrix element in the D -wave $\pi\pi$ -scattering. (c): Squared moduli of the S -matrix element in the D -wave $\pi\pi \rightarrow K\bar{K}$ process. (d): Squared moduli of the S -matrix element in the D -wave $\pi\pi \rightarrow \eta\eta$ process.

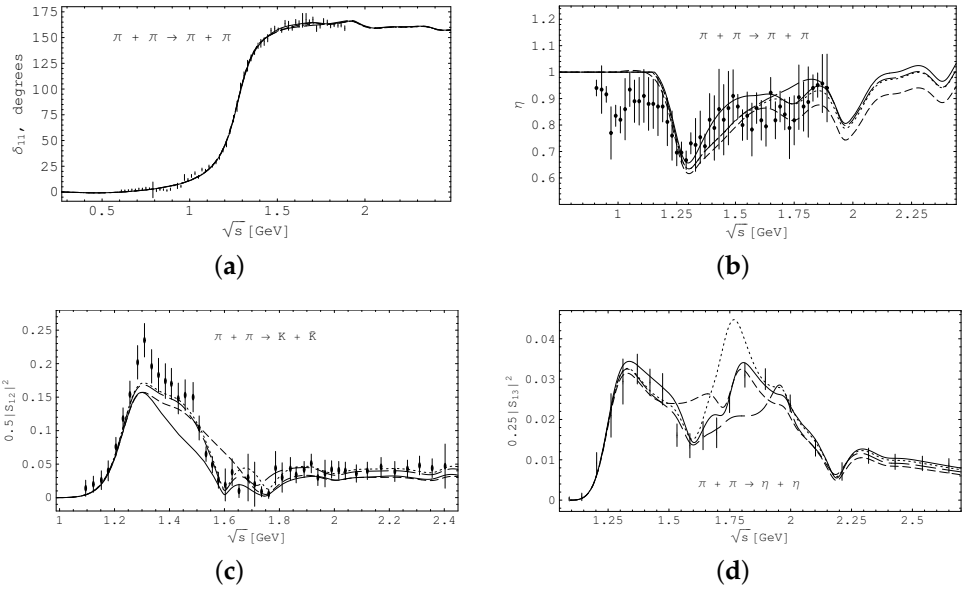


Figure 5. Scattering properties of the $\pi\pi \rightarrow \pi\pi, K\bar{K}, \eta\eta$ processes for four scenarios: (1) $f_2(1450.5)$ and $f_2(1534.7)$ states are excluded (solid line); (2) $f_2(1534.7)$ and $f_2(1719.8)$ states are excluded (dotted line); (3) $f_2(1534.7)$ and $f_2(1601.5)$ states are excluded (short-dashed line); (4) $f_2(1534.7)$ and $f_2(1760)$ states are excluded (long-dashed line). The experimental data are from Refs. [31,32]. (a): Phase shift and in the D -wave $\pi\pi$ -scattering. (b): Modulus of the S -matrix element in the D -wave $\pi\pi$ -scattering. (c): Squared moduli of the S -matrix element in the D -wave $\pi\pi \rightarrow K\bar{K}$ process. (d): Squared moduli of the S -matrix element in the D -wave $\pi\pi \rightarrow \eta\eta$ process.

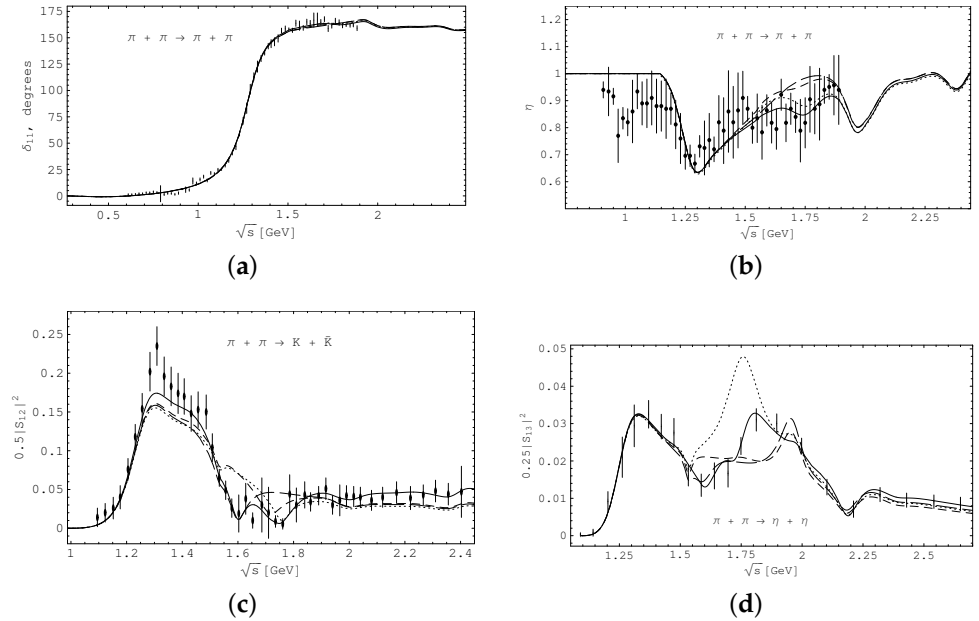


Figure 6. Scattering properties of the $\pi\pi \rightarrow \pi\pi, K\bar{K}, \eta\eta$ processes for four scenarios: (1) full result with inclusion of all relevant f_2 -resonances (solid lines); (2) $f_2(1601.5)$ and $f_2(1719.8)$ states are excluded (dotted line); (3) $f_2(1601.5)$ and $f_2(1760)$ states are excluded (short-dashed line); (4) $f_2(1760)$ and $f_2(1719.8)$ states are excluded (long-dashed line). The experimental data are from Refs. [31,32]. (a): Phase shift and in the D -wave $\pi\pi$ -scattering. (b): Modulus of the S -matrix element in the D -wave $\pi\pi$ -scattering. (c): Squared moduli of the S -matrix element in the D -wave $\pi\pi \rightarrow K\bar{K}$ process. (d): Squared moduli of the S -matrix element in the D -wave $\pi\pi \rightarrow \eta\eta$ process.

4. Conclusions

We studied the process $\gamma\gamma \rightarrow \pi^0\pi^0$ and obtained a quite satisfactory description of the data [1–3] on the cross section from the $\pi\pi$ threshold up to ≈ 2.5 GeV with a $\chi^2/\text{n.p.} \approx 1.30$.

The energy spectrum of $\gamma\gamma \rightarrow \pi^0\pi^0$ from the $\pi\pi$ -threshold to the $K\bar{K}$ -threshold is almost completely determined by the S -wave contribution and above the $K\bar{K}$ -threshold (and especially above ≈ 1.3 GeV) by the D -wave contribution. Therefore, the observed bell-shaped behaviour of the energy spectrum in the near- $\pi\pi$ -threshold region is related to the S -wave contribution, whereas the structures above 1.3 GeV to the f_2 -resonances contributing to the D -wave including their interference (see Figure 1a. From the calculated contributions of individual coupled channels to the energy spectrum of $\gamma\gamma \rightarrow \pi^0\pi^0$ (Figure 1b) we conclude that the bell-shaped behaviour of the near- $\pi\pi$ -threshold energy spectrum is mainly related to the S -wave $K\bar{K}$ intermediate state contribution. There are also large contributions by the D -wave process $\gamma\gamma \rightarrow \pi^+\pi^- \rightarrow \pi^0\pi^0$ and above ≈ 0.85 GeV by the D -wave process $\gamma\gamma \rightarrow \eta\eta \rightarrow \pi^0\pi^0$. We also notice a sizable contribution by one-pion exchange to the crossing channel of the D -wave process $\gamma\gamma \rightarrow \pi\pi \rightarrow \pi\pi$. The intermediate state $\eta\eta$ in the reaction $\gamma\gamma \rightarrow \pi^0\pi^0$ implies, of course, a preceding pair of charged particles ($\pi^+\pi^-$) in the intermediate state, that is, the process $\gamma\gamma \rightarrow \pi^+\pi^- \rightarrow \eta\eta \rightarrow \pi^0\pi^0$ and the one-pion exchange between the $\gamma\pi^+$ and $\gamma\pi^-$ vertices. This explains the noticeable contribution of the D -wave process $\gamma\gamma \rightarrow \eta\eta \rightarrow \pi^0\pi^0$.

For investigating the role of individual f_2 -resonances in $\gamma\gamma \rightarrow \pi^0\pi^0$ we switched off the different isoscalar-tensor resonances and performed for each case the combined analysis of $\gamma\gamma \rightarrow \pi^0\pi^0$, of the isoscalar S -wave processes $\pi\pi \rightarrow \pi\pi, K\bar{K}, \eta\eta$ and of the isoscalar D -wave processes $\pi\pi \rightarrow \pi\pi, (2\pi)(2\pi), K\bar{K}, \eta\eta$. Results of the analyses are shown in Table 2 and Figures 3–6. The best two variants with the $f_2(1601.5)$ and $f_2(1719.8)$ and the $f_2(1601.5)$ and $f_2(1760)$, switched off, do not give, however, a satisfactory description of the processes $\pi\pi \rightarrow K\bar{K}, \eta\eta$.

We finally completed (including previous work) a combined description of the isoscalar S -wave processes $\pi\pi \rightarrow \pi\pi, K\bar{K}, \eta\eta$, the isoscalar D -wave processes $\pi\pi \rightarrow \pi\pi, (2\pi)(2\pi), K\bar{K}, \eta\eta$, the decays of charmonia – $J/\psi \rightarrow \phi(\pi\pi, K\bar{K}), \psi(2S) \rightarrow J/\psi \pi\pi$, and $X(4260) \rightarrow J/\psi \pi^+\pi^-$, of bottomonia – $Y(mS) \rightarrow Y(nS)\pi\pi$ ($m > n, m = 2, 3, 4, 5, n = 1, 2, 3$), and of the process $\gamma\gamma \rightarrow \pi^0\pi^0$. In future we plan to include in our analysis data on the differential cross sections of the $\gamma\gamma \rightarrow \pi^+\pi^-$ process.

Author Contributions: Conceptualization, Y.S.S., P.B., T.G., R.K., V.E.L., M.N.; investigation, Y.S.S., P.B., T.G., R.K., V.E.L., M.N.; writing—original draft preparation, Y.S.S., P.B., T.G., R.K., V.E.L., M.N.; writing—review and editing, Y.S.S., P.B., T.G., R.K., V.E.L., M.N. All authors have read and agreed to the published version of the manuscript.

Funding: This work was supported in part by the Heisenberg-Landau Program, by the Votruba-Blokhintsev Program for Cooperation of Czech Republic with JINR, by the Czech Science Foundation GACR Grant No. 19-19640S (P.B.), by the Grant Program of Plenipotentiary of Slovak Republic at JINR, by the Bogoliubov-Infeld Program for Cooperation of Poland with JINR, by the BMBF (Project 05P2021, Förderkennzeichen: 05P21VTCAA), by ANID PIA/APOYO AFB180002 (Chile), by FONDECYT (Chile) under Grant No. 1191103, by ANID–Millennium Program–ICN2019_044 (Chile), and by the Polish research project with Project No. 2018/29/B/ST2/02576 (National Science Center).

Conflicts of Interest: The authors declare no conflict of interest. The funders had no role in the design of the study; in the collection, analyses, or interpretation of data; in the writing of the manuscript, or in the decision to publish the results.

References

1. Bienlein, J.K. Representation of results on $\gamma\gamma$ formation of resonances by helicity amplitude. In Proceedings of the Crystal Ball Contribution to the 9th International Workshop on Photon-Photon Collisions, La Jolla, CA, USA, 23–26 March 1992; ISSN 0418-9833.
2. Liu, Z.Q.; Shen, C.P.; Yuan, C. Z.; Adachi, I.; Asner, D.M.; Aulchenko, V. M. ; Aushev, T.; Aziz, T.; Bakich, A.M.; Bala, A.; Belous, K.; et al. Study of $e^+e^- \rightarrow \pi^+\pi^- J/\psi$ and observation of a charged charmoniumlike state at Belle. *Phys. Rev. Lett.* **2013**, *110*, 252002. [[CrossRef](#)] [[PubMed](#)]
3. Marsiske, H.; Antreasyan, D.; Bartels, H.W.; Besset, D.; Bieler, C.; Bienlein, J.K.; Bizzeti, A.; Bloom, E.D.; Brock, I.; Brockmüller, K.; et al. A measurement of $\pi^0\pi^0$ production in two photon collisions. *Phys. Rev. D* **1990**, *41*, 3324. [[CrossRef](#)] [[PubMed](#)]
4. Klein, A. Low-Energy Theorems for Renormalizable Field Theories. *Phys. Rev.* **1955**, *99*, 998. [[CrossRef](#)]
5. Garcia-Martin, R.; Moussallam, B. MO analysis of the high statistics Belle results on $\gamma\gamma \rightarrow \pi^+\pi^-, \pi^0\pi^0$ with chiral constraints. *Eur. Phys. J. C* **2010**, *70*, 155. [[CrossRef](#)]
6. Hoferichter, M.; Phillips, D.R.; Schat, C. Roy-Steiner equations for $\gamma\gamma \rightarrow \pi\pi$. *Eur. Phys. J. C* **2011**, *71*, 1743. [[CrossRef](#)]
7. Moussallam, B. Unified dispersive approach to real and virtual photon-photon scattering at low energy. *Eur. Phys. J. C* **2013**, *73*, 2539. [[CrossRef](#)]
8. Hoferichter, M.; Stoffer, P. Dispersion relations for $\gamma^*\gamma^* \rightarrow \pi\pi$: Helicity amplitudes, subtractions, and anomalous thresholds. *J. High Energy Phys.* **2019**, *7*, 73. [[CrossRef](#)]
9. Lu, J.; Moussallam, B. The $\pi\eta$ interaction and a_0 resonances in photon-photon scattering. *Eur. Phys. J. C* **2020**, *80*, 436. [[CrossRef](#)]
10. Surovtsev, Y.S.; Bydžovský, P.; Kamiński, R.; Lyubovitskij, V.E.; Nagy, M. Can parameters of f_0 mesons be determined correctly analyzing only $\pi\pi$ scattering? *Phys. Rev. D* **2012**, *86*, 116002. [[CrossRef](#)]
11. Surovtsev, Y.S.; Bydžovský, P.; Kamiński, R.; Lyubovitskij, V.E.; Nagy, M. Parameters of scalar resonances from the combined analysis of data on processes $\pi\pi \rightarrow K\bar{K}, \eta\eta$ and J/ψ decays. *Phys. Rev. D* **2014**, *89*, 036010. [[CrossRef](#)]
12. Krupa, D.; Meshcheryakov, V.A.; Surovtsev, Y.S. Uniformization of $\pi\pi$ scattering amplitude in the production channel of scalar mesons. *Yad. Fiz.* **1986**, *43*, 231.
13. Krupa, D.; Meshcheryakov, V.A.; Surovtsev, Y.S. Multichannel approach to studying scalar resonances. *Nuovo Cim. A* **1996**, *109*, 281. [[CrossRef](#)]
14. Surovtsev, Y.S.; Bydžovský, P.; Gutsche, T.; Lyubovitskij, V.E.; Kamiński, R.; Nagy, M. The scalar mesons in multi-channel $\pi\pi$ scattering and decays of the ψ and Y families. In Proceedings of the Helmholtz International School Physics of Heavy Quarks and Hadrons (HQ2013), Dubna, Russia, 15–28 July 2013; Ali, A., Bystritskiy, Y., Ivanov, M., Eds.; DESY-PROC-2013-03; Verlag Deutsches Elektronen-Synchrotron: Hamburg, Germany, 2013; pp. 284–293, ISBN 978-3-935702-82-9, ISSN 1435-8077.
15. Surovtsev, Y.S.; Bydžovský, P.; Gutsche, T.; Kamiński, R.; Lyubovitskij, V.E.; Nagy, M. Effect of the $K\bar{K}$ and $\eta\eta$ channels and interference phenomena in the two-pion and $K\bar{K}$ transitions of charmonia and bottomonia. *Phys. Rev. D* **2018**, *97*, 014009. [[CrossRef](#)]
16. Surovtsev, Y.S.; Bydžovský, P.; Kamiński, R.; Nagy, M. Light-meson spectroscopy and combined analysis of processes with pseudoscalar mesons. *Phys. Rev. D* **2010**, *81*, 016001. [[CrossRef](#)]
17. Surovtsev, Y.S.; Bydžovský, P.; Lyubovitskij, V.E.; Kamiński, R.; Nagy, M. Masses and widths of scalar-isoscalar multi-channel resonances from data analysis. *J. Phys. G Nucl. Part. Phys.* **2014**, *41*, 025006. [[CrossRef](#)]
18. Surovtsev, Y.S.; Bydžovský, P.; Lyubovitskij, V.E. On nature of the scalar-isoscalar mesons in the uniformizing-variable method based on analyticity and unitarity. *Phys. Rev. D* **2012**, *85*, 036002. [[CrossRef](#)]
19. Zyla, P.A.; Barnett, R.M.; Beringer, J.; Dahl, O.; Dwyer, D.A.; Groom, D.E.; Lin, C.-J.; Lugovsky, K.S.; Pianori, E.; Robinson, D.J.; et al. Review of Particle Physics. *Prog. Theor. Exp. Phys.* **2020**, *2020*, 083C01.
20. Anisovich, V.V.; Matveev, M.A.; Sarantsev, A.V.; Nyiri, J. Sector of the 2^{++} mesons: observation of the tensor glueball. *Int. J. Mod. Phys. A* **2005**, *20*, 6327. [[CrossRef](#)]
21. Au, K.L.; Morgan, D.; Pennington, M.R. Meson dynamics beyond the quark model: a study of final state interactions. *Phys. Rev. D* **1987**, *35*, 1633. [[CrossRef](#)]
22. Boglione, M.; Pennington, M.R. Determination of radiative widths of scalar mesons from experimental results on $\gamma\gamma \rightarrow \pi\pi$. *Eur. Phys. J. C* **1999**, *9*, 11. [[CrossRef](#)]
23. Sakurai, J.J. Theory of strong interactions. *Ann. Phys.* **1960**, *11*, 1. [[CrossRef](#)]
24. Schildknecht, D. *Generalized Vector Dominance*; Preprint DESY 73/21; Springer: Hamburg, Germany, 1973.
25. Akhiezer, A.I.; Rekalov, M.P. *Electrodynamics of Hadrons*; Naukova Dumka, Kiev, USSR: Kyiv, Ukraine, 1977.
26. Abarbanel, H.A.; Goldberger, M.L. Low-energy theorems, dispersion relations and superconvergence sum rules for Compton scattering. *Phys. Rev.* **1968**, *165*, 1594. [[CrossRef](#)]
27. Morgan, D.; Pennington, M.R. What can we learn from $\gamma\gamma \rightarrow \pi\pi, K\bar{K}$ in the resonance region. *Z. Phys. C* **1988**, *37*, 431. [[CrossRef](#)]
28. Le Couteur, K.J. The structure of a non-relativistic S -matrix. *Proc. R. Lond. Ser. A* **1960**, *256*, 115.
29. Batley, J.R.; Culling, A.J.; Kalmus, G.; Lazzeroni, C.; Munday, D.J.; Slater, M.W.; Wotton, S.A.; Arcidiacono, R.; Bocquet, G.; Cabibbo, N., et al. New high statistics measurement of K_{l4} decay form factors and $\pi\pi$ scattering phase shifts. *Eur. Phys. J. C* **2008**, *54*, 411. [[CrossRef](#)]
30. Bydžovský, P.; Kamiński, R.; Nazari, V. Dispersive analysis of the S -, P -, D -, and F -wave $\pi\pi$ amplitudes. *Phys. Rev. D* **2016**, *94*, 116013. [[CrossRef](#)]

-
31. Hyams, B.; Jones, C.; Weilhammer, P.; Blum, W.; Dietl, H.; Grayer, G.; Koch, W.; Lorenz, E.; Lutjens, G.; Manner, W.; et al. $\pi\pi$ phase shift analysis from 600 to 1900 MeV. *Nucl. Phys. B* **1973**, *64*, 134. [[CrossRef](#)]
 32. Lindenbaum, S.J.; Longacre, R.S. Coupled channel analysis of $J^{PC} = 0^{++}$ and 2^{++} isoscalar mesons with masses below 2.0 GeV. *Phys. Lett. B* **1992**, *274*, 492. [[CrossRef](#)]